JMEPEG (2010) 19:213–220
DOI: 10.1007/s11665-009-9449-z

1059-9495/$19.00

Energy Density Distribution and Temperature Closed-Loop Control in Electron Beam Processing

Xuedong Wang, Qingyu Shi, and Xin Wang

(Submitted July 25, 2008; in revised form March 11, 2009)

Various electron beam (EB) processing methods such as EB brazing, surface modification, heat treatment, etching, evaporation coating and quick manufacture, etc. require that the energy distribution and processing temperature be controlled. In this study, the energy distribution control was realized by EB scanning trajectory pattern control, and the temperature control was realized by the combined use of fuzzy logic and PID control. These were integrated into one system. To obtain large deflection angle of EB, an external deflection coil was used. The scanning trajectory pattern was the synthesization of deflections of EB in *X* and *Y* directions, and each of the deflections was controlled by an analog. Because of high energy density of the EB, and consequently high sensitivity of weldment temperature to the beam current, closed-loop control of processing temperature is indispensable, which was realized in this paper. Satisfactory transient and steady-state specifications were obtained. The brazing of a specially designed specimen verified the effectiveness of the method.

Keywords electron beam processing, fuzzy control, processing temperature, scanning trajectory pattern

1. Introduction

As a heat source used in material processing, the electron beam (EB) is characterized by its high energy density, precise control, capability of being deflected by electric/magnetic field, small focus, rapid heating and cooling, small heat input and small heat-affected zone, and ideal protection effect in vacuum. Thus, not only is EB widely used in welding nowadays, but also in other material processing methods, such as EB brazing, surface modification, heat treatment, etching, evaporation coating, and quick manufacture. The above advantages of EB processing over other conventional processing methods make it the most suitable method for the processing of the materials susceptible to temperature, active metals, or the brazing of dissimilar metals.

Although the prospect of using EB is good, two obstacles stand in the way. One is the motion control of the EB spot, which means that the focus of the EB has to be capable of moving along a predefined route, to provide the required energy density distribution on workpiece. The other is the control of temperature. Take brazing as an example. On one hand, the brazed seams are often composed of multiple curves with various shapes which require the energy density to be distributed on curves; on the other hand, the brazing temperature is an important technological parameter which needs to be controlled accurately.

Because of the high energy density of EB, the temperature of workpiece is sensitive to beam current, that is, a small variation of beam current results in large variation of temperature. Consequently, the temperature of workpiece in EB processing is difficult to control manually, which requires that a closed-loop control method be used.

In this paper, fuzzy logic is used to control the processing temperature in EB processing, because fuzzy logic is close in spirit to human thinking and can be used in the situation where exact model of a plant is not known, and we have only some experience about plant behavior (Ref 1).

The existing studies on motion control of EB spot in EB processing are limited. Bahr et al. (Ref 2) developed an EB scan and control system for high rate evaporation applications. Dupak et al. (Ref 3) presented an electron gun equipped with electronics to control the deflection of EB. As for temperature closed-loop, fuzzy control have been applied to many arc welding applications such as weld joint tracking (Ref 4), regulation of temperature (Ref 5), control of welding process (Ref 6), control of penetration (Ref 7), and modeling of bead width (Ref 8). But for EB processing, the existing studies on temperature closed-loop are seldom seen.

In this paper, an EB processing system was constructed which has the abilities of synchronous control of EB scanning trajectory and workpiece temperature.

The control system designed is composed of an EB welder, industrial control computer, programmable controller, power amplifiers, infrared thermometer, deflection coil, data acquisition device, AD/DA converters and control software, etc., as shown in Fig. 1. In the figure, the entire system is divided into five subsystems of functions—process control of EB processing, closed-loop control of temperature, data acquisition and handling, scanning trajectory pattern control, and energy density control.

In the following sections, except the process control of EB processing, all the other four subsystems will be discussed, since the process control of EB processing can be found in any references on EB welding.

Xuedong Wang, Qingyu Shi, and **Xin Wang**, Department of Mechanical Engineering, Tsinghua University, Beijing, China. Contact e-mail: wxue2004@yeah.net.

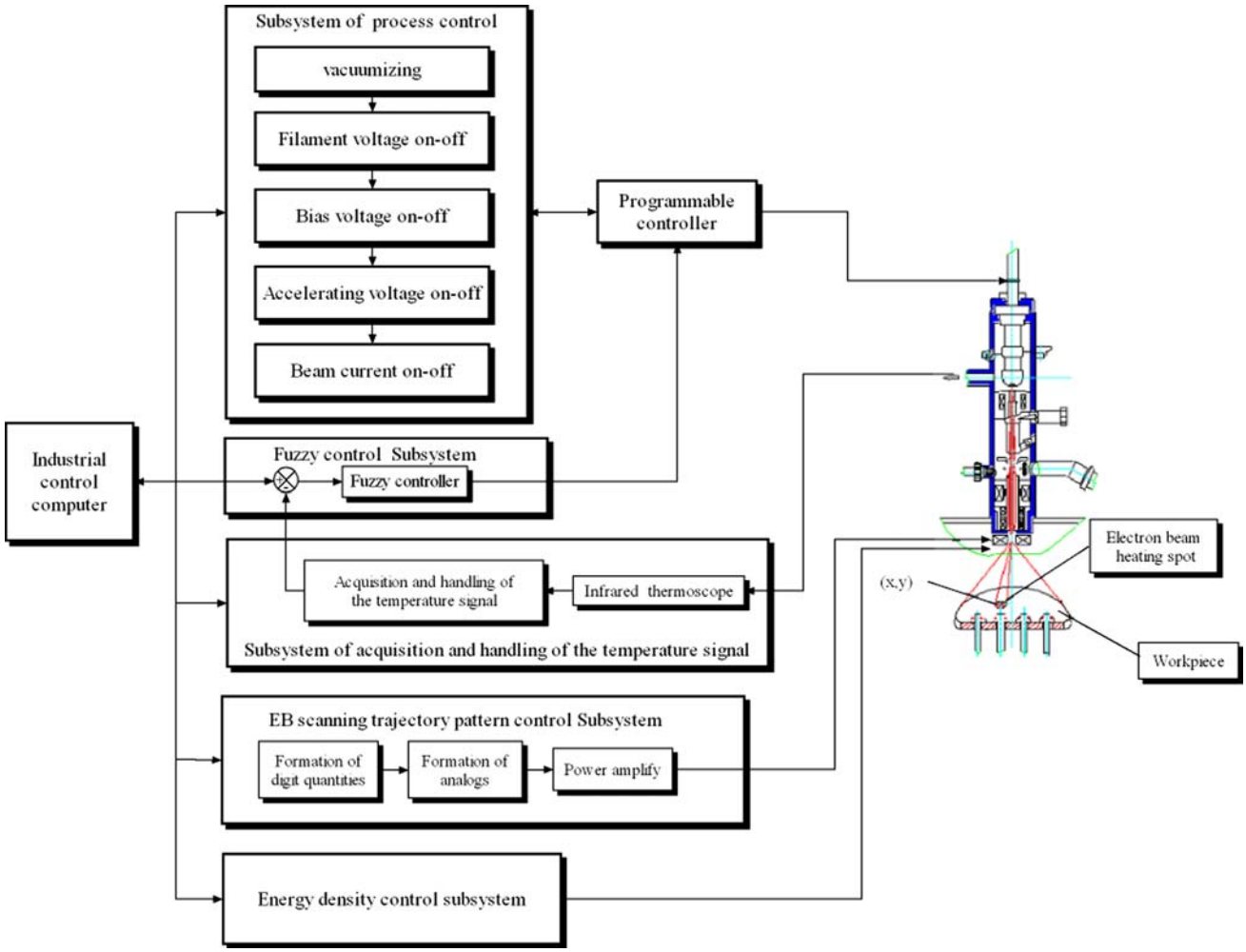

Fig. 1 Schematic diagram of the control system

2. Control of Scanning Trajectory and Energy Density Distribution

2.1 Control of Scanning Trajectory

Although in electron gun of an EB welder, there is an internal deflection coil, limited by the structure of the electron gun, the maximum deflection angle that can be generated by this coil is quite limited. Thus, this deflection can only generate stirring effect on molten pool during welding. Hence, to expand the scanning scope, an external deflection coil was adopted in this study, which was mounted out of the electron gun, and beneath the outlet of the gun. The coil has two magnetic poles, controlling the deflection of the EB in X and Y directions, respectively. The dimension of the coil is $\varnothing 102 \times 65$ mm, the frequency range is 0-15 KHz, and the deflection angle range is $-18°$ to $+18°$.

The scanning trajectory pattern is designed according to the requirement of energy density distribution of EB processing. Based on the trajectory pattern, analogs for generating the alternating magnetic fields in the deflection coil are calculated by the program running in the industrial control computer. Since the deflection coil is composed of two windings, X winding and Y winding, which are perpendicular to each other, two analogs are needed to be input into the X and Y windings, respectively. The X, Y quantities are obtained by the software developed by the authors. They are digitals at the beginning, and then converted to analogs by D/A converters. After the two analogs are formed, and magnified by the power amplifiers, they are input into the X and Y windings to generate the alternating magnetic fields in X and Y directions. The alternative frequencies of the magnetic fields are adjusted by the program and the program-controlled D/A converters. When the EB passes through the deflection coil, it will be driven to deflect by the alternating magnetic fields. As a result, the spot of the EB scans along predefined trajectory.

Examples of scanning trajectories are shown in Fig. 2, in which, four kinds of patterns are presented; the ones in the upper row are the scanning trajectories calculated by the program, and those in the lower row are the photographs of the corresponding scanning trajectories.

2.2 Control of Energy Density Distribution

The control of scanning trajectory and energy density distribution are the same in essence. Because the latter can give us more chances in terms of effectiveness and flexibility, so it is discussed separately.

Take the three different patterns of energy density distribution shown in Fig. 3-5, for example. In Fig. 3, (a) is a

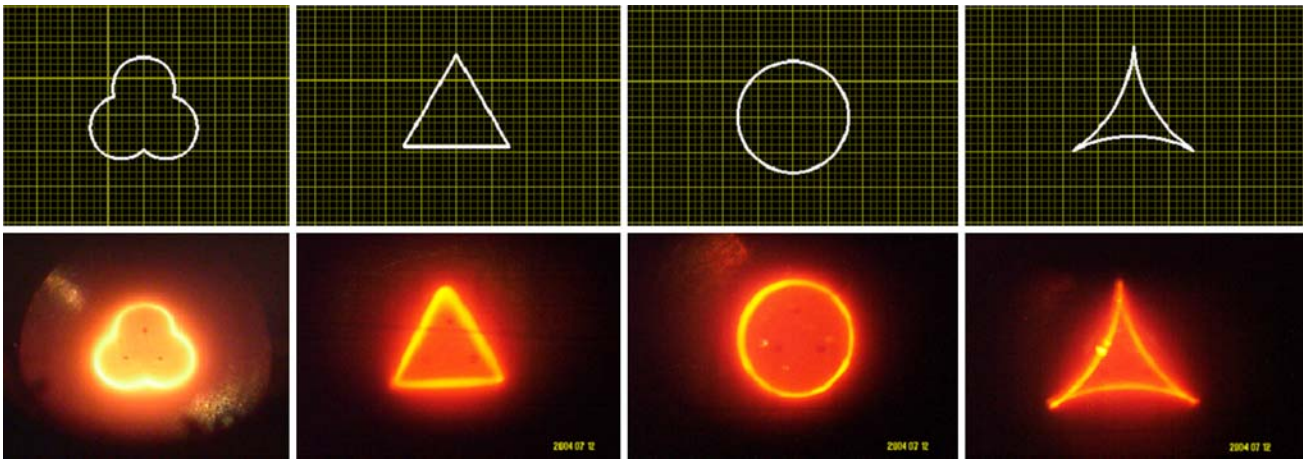

Fig. 2 Examples of scanning trajectories

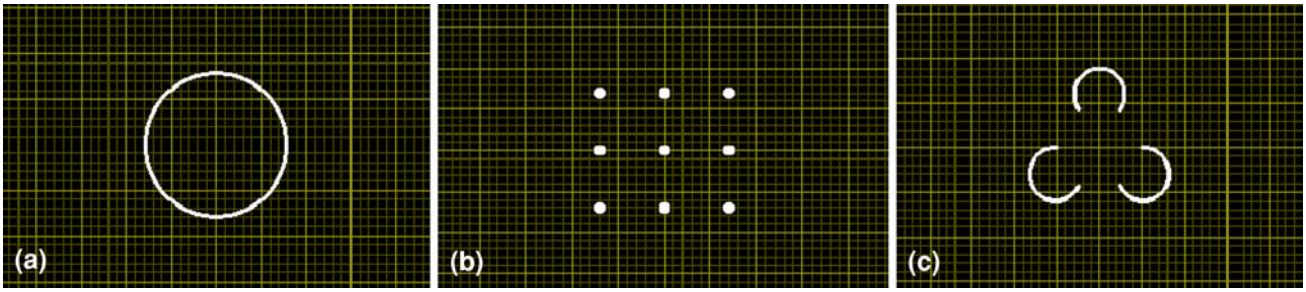

Fig. 3 Three different patterns of energy density distribution

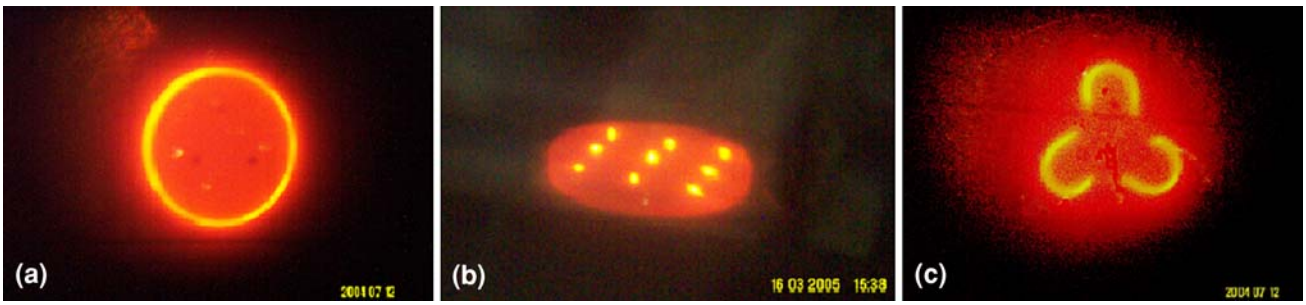

Fig. 4 The obtained scanning trajectory patterns

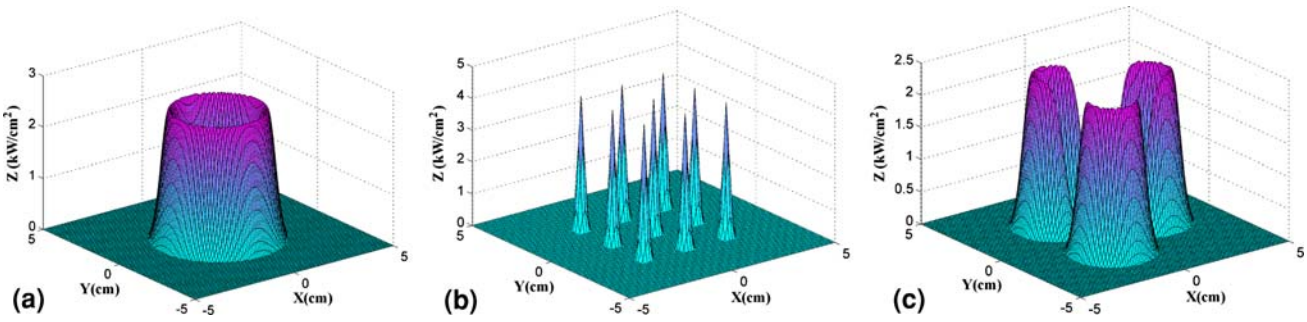

Fig. 5 The calculated energy density distribution of the three kinds of scanning trajectories

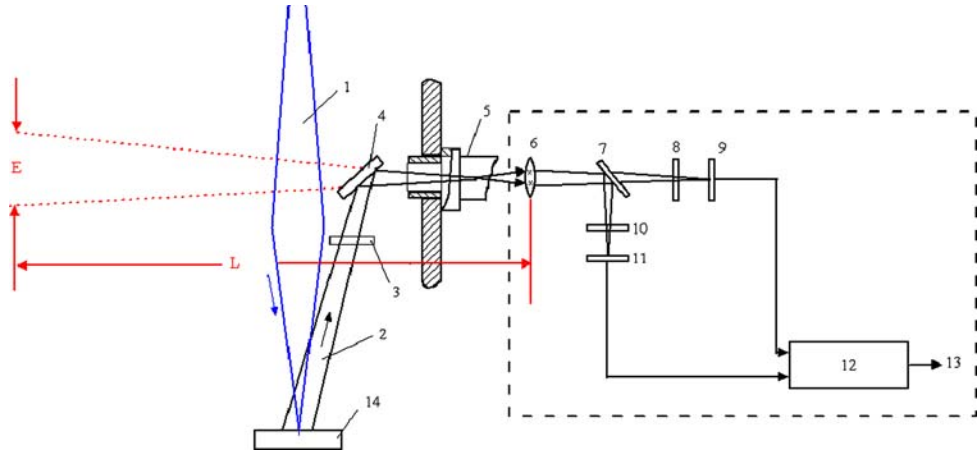

Fig. 6 The sketch of temperature detection by two-color infrared thermometer. 1—incident electron beam, 2—infrared radiation, 3—protection lens, 4—reflecting mirror, 5—observation window, 6—objective, 7—dichroic mirror, 8—light filter 1, 9—detector 1, 10—light filter 2, 11—detector 2, 12—microprocessor, 13—temperature reading, 14—weldment

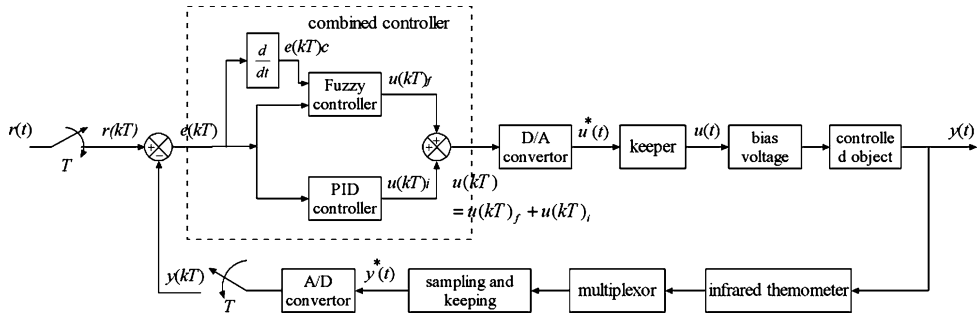

Fig. 7 The schematic diagram of the fuzzy control system

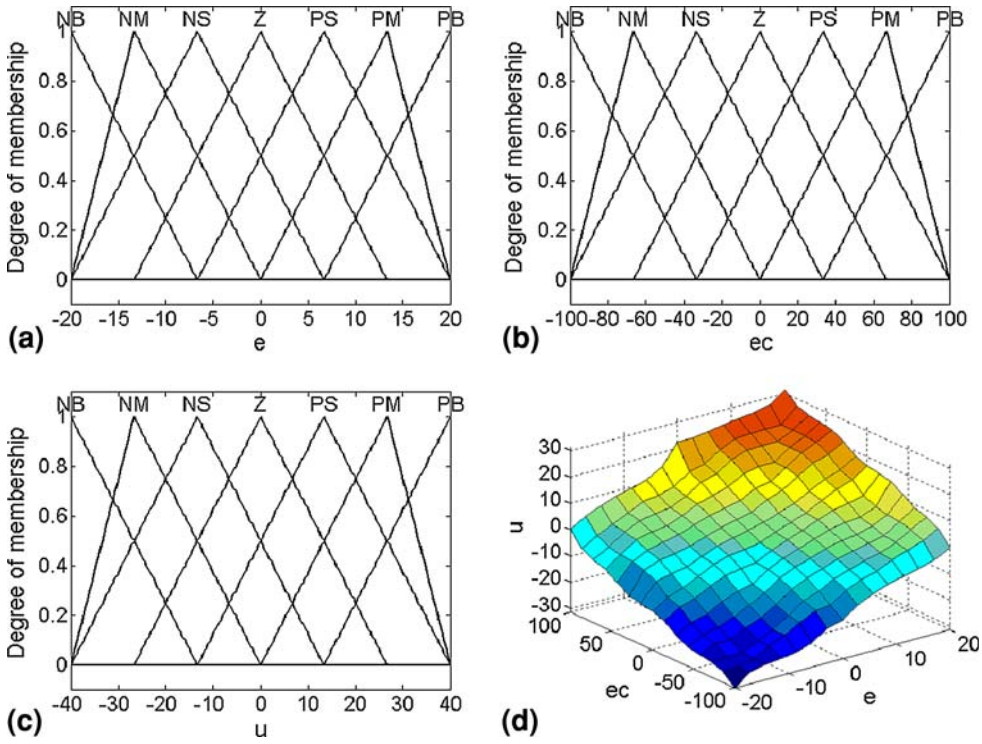

Fig. 8 The membership functions of the input and output variables and the output characteristic

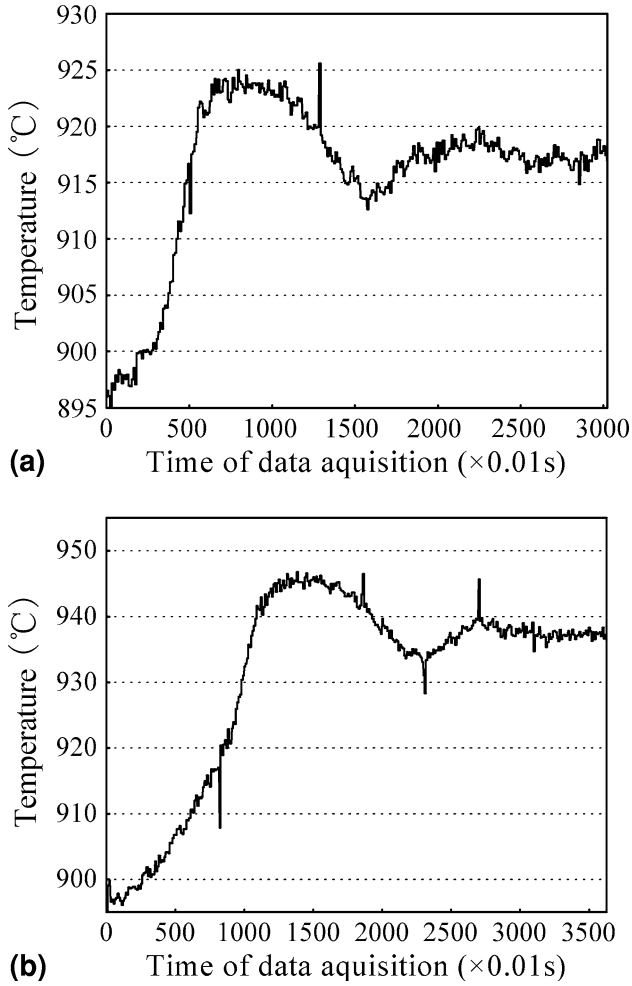

Fig. 9 The responses of the fuzzy control system

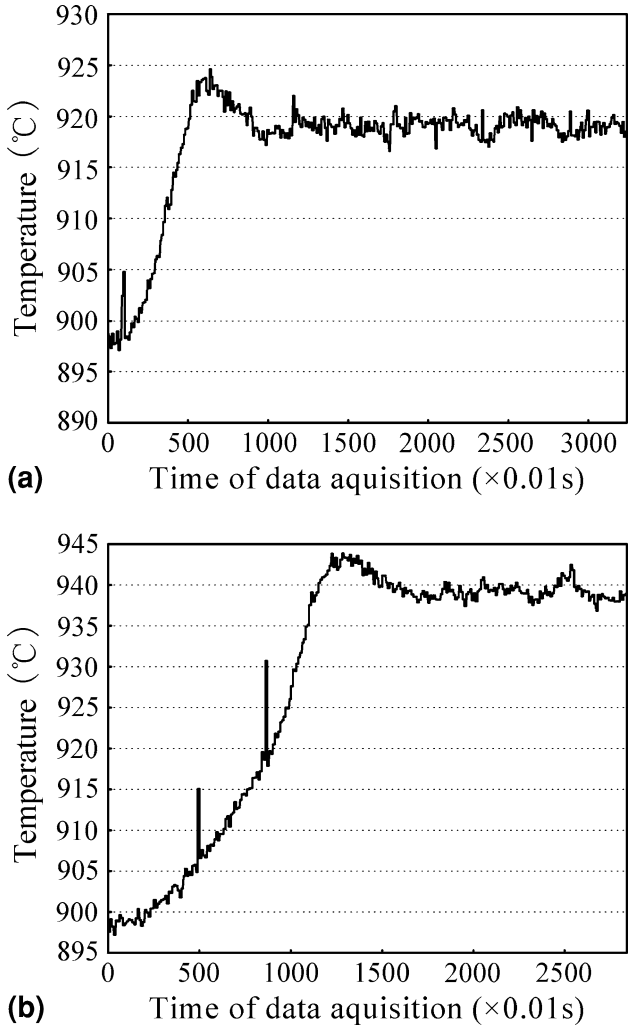

Fig. 10 The responses of the combined fuzzy-PID controller

continuous scanning trajectory; in (b), energy concentrates in some point locations; and (c) is a discontinuous scanning trajectory pattern composed of multiple curves. In Fig. 4, the corresponding scanning trajectories represent exactly the energy density distribution requirements of Fig. 3. The calculated energy density distribution are given in Fig. 5(a-c).

3. Temperature Closed-Loop Control

3.1 Temperature Detection

One important element in realization of temperature closed-loop control is the temperature detection, which is performed synchronously with the other functions in the system. In this paper, a two-color infrared thermometer is used to detect the temperature of the brazed seam, as shown in Fig. 6. The infrared radiation of the brazed seam passes through the protection lens and the observation window of the vacuum chamber, entering the thermometer through the objective. In the thermometer, the infrared radiation is separated into two beams with wavelengths of λ_1 and λ_2, respectively, by the dichroic mirror. Then, the energies of the radiations are transformed into electrical signals by two detectors, respectively. Finally, the electrical signals are entered into the microprocessor of the thermometer, which gives the temperature signals according to the energy ratio of the two beams of radiation. One of the advantages of the two-color thermometer over ordinary infrared thermometers is that the accuracy of temperature measurement will not be influenced by attenuation of infrared radiation (Ref 9).

Table 1 The transient specifications of the control system with combined controller

Figure	Controller	Temperature change, °C	Overshoot, °C	Peak time, s	Rising time, s	Settling time, s
10(a)	Fuzzy-PID	900 → 920	4	6.2	5	4.5
10(b)	Fuzzy-PID	900 → 940	4	13.5	12.5	12

3.2 Combined Fuzzy-PID Control

Besides temperature measurement, how to adjust EB power is another crucial factor in realization of temperature closed-loop control.

In electron guns, the acceleration voltage is applied between the anode and the cathode, and the latter has negative electric potential relative to the former. When electrons are emitted

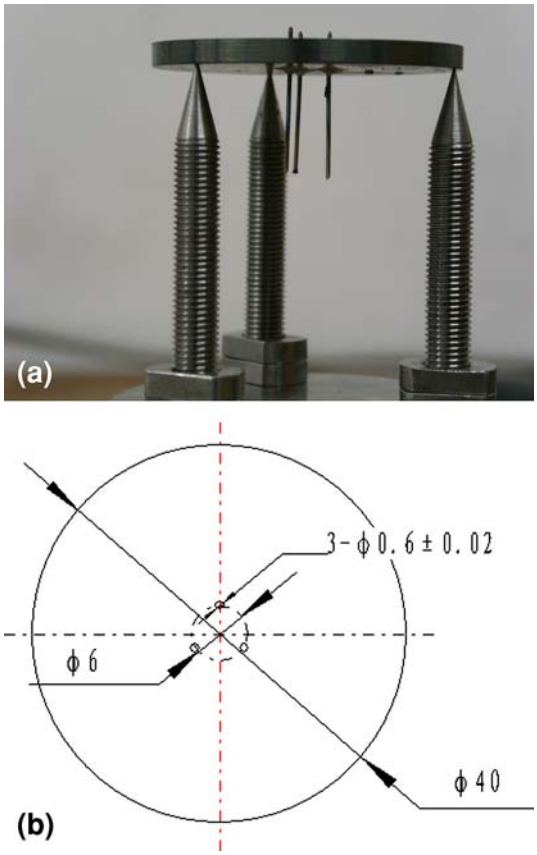

Fig. 11 The photograph and dimension of the specimen

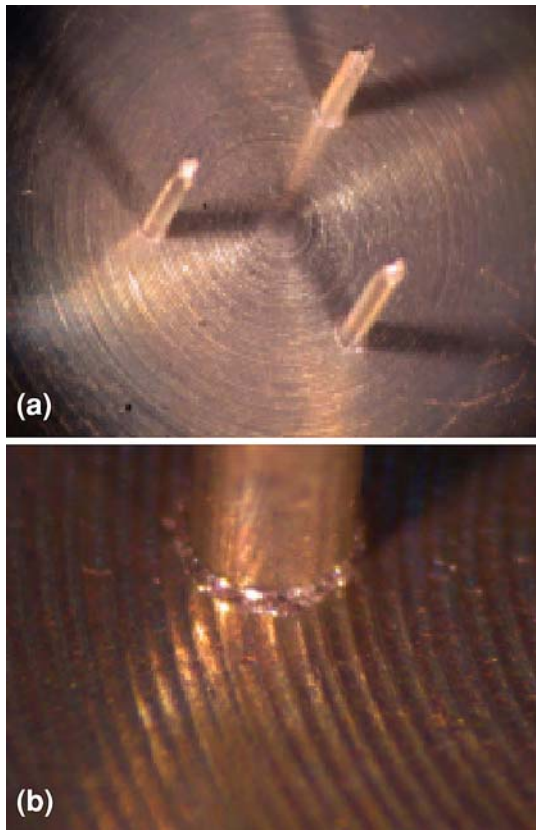

Fig. 12 The brazed joint

from the cathode, they are accelerated by the acceleration voltage. In tripolar electron guns, there is a grid electrode equipped between the anode and the cathode. The grid electrode is applied a negative voltage, and the absolute value of it is larger than that of the cathode voltage. So the grid electrode applies a repelling force to the electrons from the cathode. The larger the absolute value of the grid voltage is, the larger the repelling force is, and the fewer electrons pass through the grid electrode per unit time. In short, increment/reduction of the absolute value of the grid bias voltage leads to the reduction/increment of the beam current under conditions when a fixed accelerating voltage is applied. With the help of this characteristic, a fuzzy closed-loop control system is constructed to realize the real-time regulation of beam current. The schematic diagram of the system is shown in Fig. 7. The PID controller in the figure will not be discussed at this stage.

In the figure, $r(t)$ is the set value of temperature, and T is the sampling period. $r(kT)$ is the transient value of the input signal $r(t)$, $y(kT)$ is the feedback signal, i.e., the detected temperature signal of the workpiece. Subtraction of $y(kT)$ from $r(kT)$ yields $e(kT)$, which is known as deviation signal, i.e., the difference between the set value and the actual value of temperature. $u(kT)_f$ is the output of the fuzzy controller, which is converted to analog $u(t)$ by D/A converter and keeper. $u(t)$ is used to adjust the bias voltage.

The fuzzy controller has two input terminals, $e(kT)$ and $e(kT)c$. $e(kT)c$ is derivative of $e(kT)$, which represents the change rate of the temperature deviation.

The membership functions used by the fuzzy controller are shown in Fig. 8(a-c), in which, e, ec, and u correspond to $e(kT)$, $e(kT)c$, and $u(kT)_f$, respectively. The output characteristic of the fuzzy controller is shown in Fig. 8(d), which suggests that the output is quite smooth with no abrupt change.

The responses of the fuzzy control system to step signals are shown in Fig. 9, in which, two temperature step signals were tested, 20 °C (Fig. 9a) and 40 °C (Fig. 9b). The steady-state values of temperature should be 920 and 940 °C, whereas the actual values were 917.5 and 937 °C, respectively, which indicates that steady-state errors exist. The errors are 2.5 and 3 °C, respectively.

Usually, in fuzzy control systems, steady-state error often exists (Ref 10). To eliminate the steady-state error, a PID controller was used together with the fuzzy controller to form a combined controller, as shown in Fig. 7. The design of the PID controller can be found in Ref 11. Only one of the two controllers is activated at one time according to a threshold value of $e(kT)$, which is set as 5 °C in this paper. In the case that $e(kT)$ is larger than the threshold, the fuzzy controller is active; in the case that $e(kT)$ is smaller than the threshold, the fuzzy controller is deactivated and the PID controller is activated.

The responses of the system with combined controller are shown in Fig. 10. The transient specifications are listed in Table 1. It can be seen from Fig. 10 that the steady-state errors have been eliminated by and large. Table 1 indicates that the dynamic performances are satisfactory: small overshoot, short settling time. It is quite a surprise that the settling time is shorter than the rising time, which means that the responses do not need any accommodation at all.

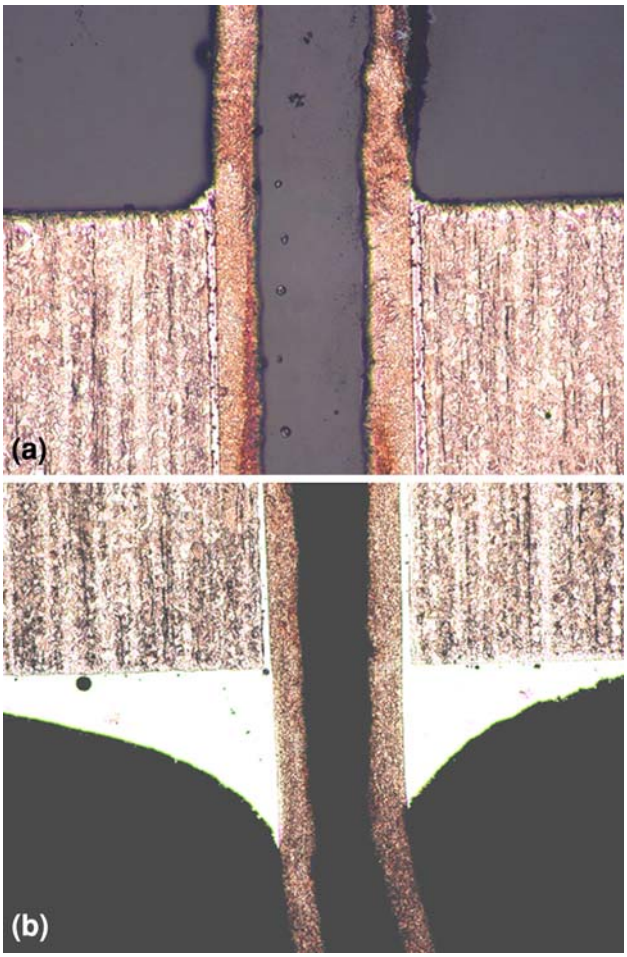

Fig. 13 The cross section photograph of the brazing joint 50×

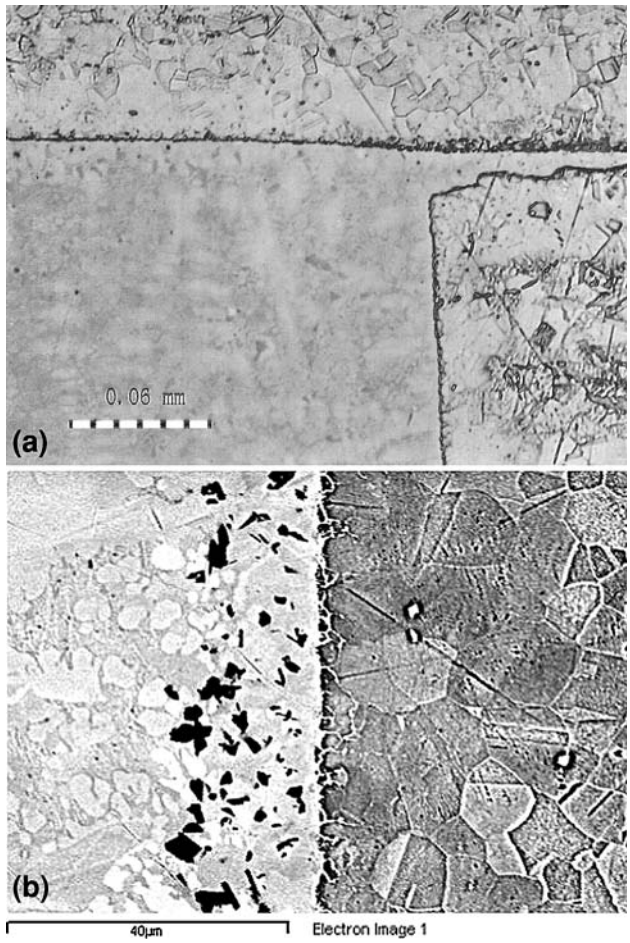

Fig. 14 The microstructure and backscattered electron image of the brazed joint

4. EB Brazing Experiments

To verify the effectiveness of the system, an EB brazing experiment was performed, though this system is not confined to brazing. A special specimen was designed for the experiment, as shown in Fig. 11.

In Fig. 11, (a) is the photograph of the specimen (the specimen is supported by three core clampers). The specimen is composed of a circular plate and three capillary tubes. There are three holes in the circular plate. The capillary tubes are put in the holes and brazed with the plate. The plate is 3 mm thick, and the wall thickness of the capillary tube is 0.15 mm. The other dimensions of the specimen are shown in Fig. 11(b).

The material of the capillary tubes and the plate is 1Cr18Ni9Ti (in wt.%): 17-19%Cr, 8-11%Ni, 5%Ti (with ≤0.12%C, ≤1.0%Si, and ≤2.0%Mn). The brazing filler metal is Pulverous BNi-2 with the following composition: 7.33%Cr, 3.3%Fe, 2.93%B, 4.02%Si (with 0.02%O, 0.02%C, and 0.08%Co). The brazing temperature was 1000 °C. The scanning trajectory pattern used is the first left one in Fig. 2.

Figures 12 and 13 are the macroscopic photographs of the obtained brazed joint, and the metallurgical structures are shown in Fig. 14(a) and (b).

The macroscopic observation shows that the surface of the brazed seam is uniform and smooth, the filler metal wetted the walls of the capillary tubes very well, the brazed rate is 100%, and the fillet size is consistent. No erosion, blockage, and leakage were found in the macroscopic metallographic examination. In Fig. 14(a), the upper part is the wall of the capillary tube, the lower-left part is the filler metal, and the lower-right part is the plate metal. The microscopic observation shows that the grains of the base metal are small, and no erosion has occurred. In Fig. 14(b), the view on the left is metallurgical structure of the filler metal, and the view on the right side is the structure of the plate. From the figure, one can see that the diffusion layer has been formed, which is about 15-20 μm thick.

5. Conclusion

The following conclusions are drawn:

1. Combined Fuzzy-PID control method can be used in temperature closed-loop control of EB processing. The transient and steady-state specifications of the control system are satisfactory.
2. EB scanning trajectory control and temperature closed-loop control can be integrated in EB processing system and work synchronously.

3. The controllability of the scanning trajectory pattern and temperature was shown to provide feasibility of EB brazing, similar results may be expected for surface heat treatment and modification, etching, evaporation coating and quick manufacture, etc. especially for the processing of the materials sensitive to temperature.

References

1. B.S. Butkiewicz, Steady-State Error of a System with Fuzzy Controller, *IEEE Trans. Syst. Man Cybernet. B*, 1998, **28**(6), p 855–860
2. M. Bahr, G. Hoffmann, R. Ludwig, and G. Steiniger, New Scan and Control System (Escosys™) for High Power Electron Beam Techniques, *Surf. Coat. Technol.*, 1998, **98**(1–3), p 1211–1220
3. J. Dupak, I. Vlcek, and M. Zobac, Electron Gun for Computer-Controlled Welding of Small Components, *Vacuum*, 2001, **62**(2–3), p 159–164
4. Z. Bingul, G.E. Cook, and A.M. Strauss, Application of Fuzzy Logic to Spatial Thermal Control in Fusion Welding, *IEEE Trans. Ind. Appl.*, 2000, **36**(6), p 1523–1530
5. K.S. Boo and H.S. Cho, A Self-Organizing Fuzzy Control of Weld Pool Size in GMA Welding Processes, *Control Eng. Pract.*, 1994, **2**(6), p 1007–1018
6. L. Di, T. Srikanthan, R.S. Chandel, and I. Katsunori, Neural-Network-Based Self-Organized Fuzzy Logic Control for Arc Welding, *Eng. Appl. Artif. Intel.*, 2001, **14**(2), p 115–124
7. C.H. Tsai, K.H. Hou, and H.T. Chuang, Fuzzy Control of Pulsed GTA Welds by Using Real-Time Root Bead Image Feedback, *J. Mater. Process. Technol.*, 2006, **176**(1–3), p 158–167
8. Y. Xue, I.S. Kim, J.S. Son, C.E. Park, H.H. Kim, B.S. Sung, I.J. Kim, H.J. Kim, and B.Y. Kang, Fuzzy Regression Method for Prediction and Control the Bead Width in the Robotic Arc-Welding Process, *J. Mater. Process. Technol.*, 2005, **164**, p 1134–1139
9. B. Muller and U. Renz, Development of a fast fiber-optic two-color pyrometer for the temperature measurement of surfaces with varying emissivities, *Rev. Sci. Instrum.*, 2001, **72**(8), p 3366–3374
10. J.C. Quadrado and J. Fernando Silva, On the Elimination of Steady-State Errors with an ''Elastic'' Fuzzy Position Controller for Motor Drives, *Proceedings of the IECON '93, International Conference on Industrial Electronics, Control, and Instrumentation, 1993*, vol. 1, 1993, p 194-199
11. X.-D. Wang, Q.-Y. Shi, and X. Wang, New Vacuum Electron Beam Processing Method Based on Temperature Closed-Loop Control, *Vacuum*, 2009, **83**(5), p 857–864